HYDROLOGICAL PROCESSES
Hydrol. Process. **24**, 2724–2737 (2010)
Published online 28 June 2010 in Wiley Online Library
(wileyonlinelibrary.com) DOI: 10.1002/hyp.7686

Depth-averaged, spatially distributed flow dynamic and solute transport modelling of a large-scaled, subtropical constructed wetland

Joong-Hyuk Min[1]* and William R. Wise[2]

[1] *Soil and Water Science Department, University of Florida, Gainesville, FL 32611, USA*
[2] *Department of Civil and Coastal Engineering, University of Florida, Gainesville, FL 32611-6580, USA*

Abstract:

Constructed wetlands are being utilized worldwide to effectively reduce excess nutrients in agricultural runoff and wastewater. Despite their frequency, a multi-dimensional, physically based, spatially distributed modelling approach has rarely been applied for flow and solute transport in treatment wetlands. This article presents a two-dimensional hydrodynamic and solute transport modelling of a large-scaled, subtropical, free water surface constructed wetland of about 8 km^2 in the Everglades of Florida, USA. In this study, MIKE 21 was adopted as the basic model framework. Field monitoring of the time series hydrological and chloride data, as well as spatially distributed data such as bathymetry and vegetation distribution, provided the necessary model input and testing data. Simulated water level profiles were in good agreement with the spatio-temporal variations of measured ones. On average, the root-mean-square error of model calibration on annual water level fluctuations was 0·09 m. Manning's roughness coefficients for the dense emergent and submerged aquatic vegetation areas, which were estimated as a function of vegetation type, ranged from 0·67 to 1·0 and 0·12 to 0·15 $s/m^{1/3}$, respectively. The solute transport model calibration for four monitoring sites agreed well with the measured annual variations in chloride concentration with an average percent model error of about 15%. The longitudinal dispersivity was estimated to be about 2 m and was more than an order of magnitude higher than the transverse one. This study is expected to play the role of a stepping stone for future modelling efforts on the development and application of more advanced flow and transport models applicable to a variety of constructed wetland systems, as well as to the Everglades stormwater treatment areas in operation or in preparation.

KEY WORDS free water surface constructed wetland; hydrodynamics; solute transport; distributed modelling; hydraulic resistance; dispersivity

Received 6 September 2009; Accepted 9 March 2010

INTRODUCTION

The Everglades is an internationally recognized subtropical wetland ecosystem in South Florida. Historically, it was a vast oligotrophic freshwater wetland that covered all but the most easterly land of South Florida before the 1900s (Chimney and Goforth, 2001). Since then, this ecologically unique wetland system has been adversely impacted by the altered hydrology which was originally intended for flood control and the influx of nutrient-rich runoff generated from agricultural activities and urban development (Newman and Lynch, 2001). Since Florida's 1994 Everglades Forever Act was passed, several construction, research and regulation activities for restoring the remaining Everglades ecosystem have been conducted, including application of constructed wetlands referred to as stormwater treatment areas (STAs) and implementation of best management practices (Guardo *et al*., 1995; Goforth, 2001). Use of constructed wetlands for nutrient removal, particularly phosphorus in South Florida, from nutrient-enriched upstream agricultural runoff or wastewater has been extensively recognized as one of the most feasible and cost-effective technologies in the world (Mitsch, 1994; Gearheart, 1999; Kivaisi, 2001). The Everglades STAs comprise the largest constructed wetland system in the world to date (Chimney and Goforth, 2001).

The most important factor sustaining the structure and function of wetland systems is the flow (Hammer, 1989; Arnold *et al*., 2001). Understanding flow characteristics in constructed wetlands is also essential because it determines the availability of pollutants for assimilation by biota and sorption by soils. In addition, it significantly changes temporally because storm events in the wet season can generate huge runoff, and drought in the dry season can result in the wetland surface going almost dry. In spite of their importance, wetland flow dynamics traditionally have been assumed to operate under unrealistic hydraulic conditions such as steady-state and plug flow, which are based on unrealistic physical settings such as rectangular wetland shape, constant flat bathymetry (slope) and a single value of flow resistance. These are the inherent limitations of traditional wetland flow models, which depend mainly on one-dimensional (1D), conceptual and parameter-lumped modelling approaches. In

* Correspondence to: Joong-Hyuk Min, Soil and Water Science Department, University of Florida, 2169 McCarty Hall, Gainesville, FL 32611, USA. E-mail: jhmin@ufl.edu

addition, it is neither easy to find the physical meanings of the key parameters associated with pollutant removal nor possible to independently estimate the impacts of various physical and ecological factors affecting the flow and solute transport. Kadlec (2000) suggested that new paradigms are required that incorporate the ability to describe short-circuiting and spatial distribution of vegetation, indicating the inadequacy of traditional phosphorus retention modelling approaches. Even though these traditional wetland modelling approaches have been very useful as management modelling tools during the early stage of system development and as a predictive tool of long-term average treatment efficiency, spatially distributed numerical modelling approaches for flow and solute transport in constructed wetlands are necessary to more systematically understand and predict the heterogeneities of internal hydrodynamic and transport processes, overcoming the critical shortcomings of previous modelling efforts (Moustafa and Hamrick, 2000; Min and Wise, 2009).

Multi-dimensional, physically based, spatially distributed flow dynamics/transport modelling approaches have been suggested as some alternatives (Feng and Molz, 1997; Persson *et al*., 1999; Jawitz *et al*., 2008). However, several shortcomings of these modelling approaches have been also reported: (1) the requirements of enormous input data and physical parameters, (2) complexity of model calibration/validation, (3) model uncertainty and (4) requirement of huge time and effort (Kadlec and Hammer, 1988; Van Nes and Scheffer, 2005; Fernandez *et al*., 2006). In spite of the shortcomings, these approaches have been widely applied in a variety of water bodies (Ji, 2008), such as streams/rivers (Kronvang *et al*., 1999; Cook *et al*., 2003; Conaway and Moran, 2004; McMichael *et al*., 2006), lakes (Chen, 1994; Jin *et al*., 2001; Chen and Sheng, 2005), bays/estuaries/lagoons (Johnson *et al*., 1993; Chen, 1994; Swain *et al*., 2004; Ferrarin and Umgiesser, 2005; Park *et al*., 2005; Zacharias and Gianni, 2008) and natural wetlands (Tsanis *et al*., 1998; Thompson *et al*., 2004; Cui *et al*., 2005; Langevin *et al*., 2005; Persson, 2005). This is attributed to the fact that they allow the inclusion of important physical modelling aspects, such as heterogeneity and variability, and produce testable predictions, which cannot be incorporated in historically simple wetland models (Van Nes and Scheffer, 2005). This is also due to recent progress in computer technology, which allows use of both temporal and spatial data resulting in more sophisticated numerical models. However, these approaches have rarely been applied to flow and solute transport in large-scaled, subtropical constructed wetlands (Guardo and Tomasello, 1995; Moustafa and Hamrick, 2000). The previous two models were used to analyse the performance of the Everglades Nutrient Removal Project (Guardo and Tomasello, 1995) and successfully simulated the interior water surface elevations and chloride levels (Moustafa and Hamrick, 2000), although commonly applied key modelling parameters were assumed or not explicitly determined in those studies.

This study presents the development and application of a linked model for flow and solute transport, with field data collected at the northern flow way of STA 5 in South Florida. The objectives of this study were (1) to develop a depth-averaged, spatially distributed flow dynamic and solute transport model using the MIKE 21 hydrodynamics (HD) and advection–dispersion (AD) modelling framework, which can be easily applied to various free water surface constructed wetland systems ranging from small-scale ponds to large-scale treatment wetlands and (2) to suggest model-based values (or ranges) of key parameters commonly applied, but not extensively studied, in areas covered by various wetland vegetation, in flow dynamics and solute transport models (e.g. hydraulic roughness coefficients and dispersivities) through model testing, which may be directly or indirectly available to free water surface constructed wetland systems similar to the South Florida STAs. This study is expected to be a stepping stone for future modelling efforts for the development of more advanced flow and nutrient dynamics models applicable to a variety of constructed wetland systems as well as to the Everglades STAs in operation or in preparation.

SITE DESCRIPTION

A regional map showing the location of STA 5 and significant features in the South Florida landscape is presented in Figure 1a. STA 5, one of six free water surface constructed wetlands, is located in Hendry County, Florida. It extends from the L-2 Canal to the west to the Rotenberger Wildlife Management Area to the east (Figure 1b). The antecedent land use of STA 5 was agricultural cropland for sugarcane (Goforth, 2005). STA 5 receives untreated agricultural stormwater runoff from the C-139 Basin via the Canal L-2. If runoff exceeds the hydraulic capacity of STA 5, flow is diverted away. Treated water is collected and discharged either to the Rotenberger Wildlife Management Area or to the Miami Canal (Figure 1b). Seepage collection canal is located along the northern boundary of STA 5 in order to return seepage via a pump station (G349A) to the upstream treatment cell (Figure 1b). The role of these hydraulic structures is to avoid STA 5 dry-out under drought condition.

A schematic of the modelled area, STA 5 northern flow way, showing the flow and vegetation patterns as well as the hydraulic structures, is illustrated in Figure 1b. It consists of two consecutively linked treatment cells (Cells 1A and 1B), which are divided by a perimeter levee and connected by culverts and weirs. They contain approximately 338 and 494 ha of effective treatment area, respectively [South Florida Water Management District (SFWMD, 2000)]. Water enters the flow way from the west (Canal L-2) and flows by gravity through the treatment area to the east (discharge canal). Within the flow way, there are two dominant vegetation communities: emergent aquatic vegetation (EAV) and submerged

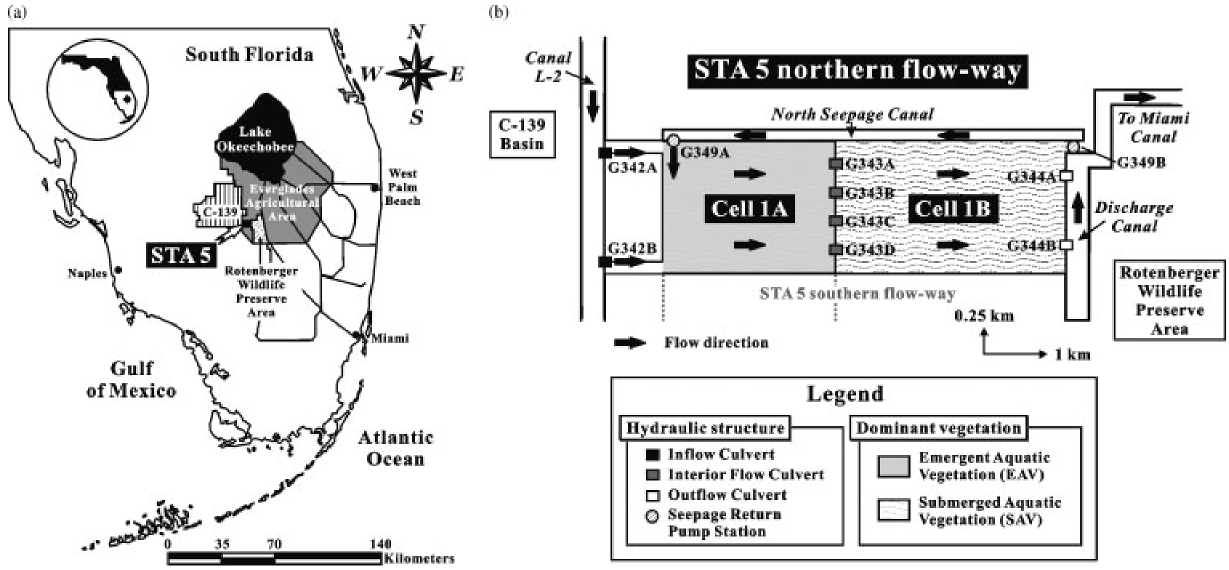

Figure 1. Location map of the study area and a schematic. (a) Regional map showing location of STA 5 and significant features in the South Florida landscape. (b) Schematic of the STA 5 northern flow way showing the flow and vegetation patterns as well as the hydraulic structures

Table I. Vegetation type of STA 5 northern flow way

Type of vegetation habitat	Dominant vegetation species	Areal ratio (%)	
		Cell 1A	Cell 1B
Emergent	Cattail, mixed cattail and mixed graminoids	39·1	0·2
Floating	Floating/floating attached emergents	1·2	0·0
Shrub	Primrose willow, mixed cattail and primrose willow	18·2	0·0
Open water with or without vegetation	—	12·1	3·8
Open water with *Hydrilla*	*Hydrilla, Hydrilla* with periphyton	29·4	96·0

Source: STA 5 vegetation map as a format of GIS shapefile (Nick Miller, Inc., 2006).

aquatic vegetation (SAV). Cells 1A and 1B are EAV- and SAV-dominant treatment cells, respectively. EAV species found in Cell 1A are typically *Typha* spp. (cattail) and *Ludwigia* spp. (primrose willow); Cell 1B is mostly comprised of invasive exotic SAV species, *Hydrilla verticillata* and periphyton (Table I). As shown in Figure 1b, inflow to the northern flow way from the Canal L-2 is controlled by two gated concrete box inflow culverts (G342A and G342B) and a pump station for seepage return (G349A). The flow induced through the culverts is conveyed through spreader canals, which separate the higher topographic elevation area (west of the spreader canals; dry most of the time during normal operation) from the upstream treatment cell. The water level of Cell 1A is also controlled by four concrete box culverts with upstream weirs (G343A to G343D) located on the middle levee between Cells 1A and 1B. Likewise, water level of Cell 1B is controlled by two gated concrete box outflow culverts (G344A and G344B).

More detailed descriptions on the operational and management history, as well as the physical characteristics, of STA 5 are contained in the chapters detailing STA performance in the annual South Florida Environmental Reports (Pietro *et al.*, 2009) and other SFWMD documents (SFWMD, 2000; Goforth, 2005).

METHODS

Modelling framework: MIKE 21

MIKE 21 was developed by the Danish Hydraulic Institute (DHI) for two-dimensional (2D) free surface flows occurring in coastal hydraulic areas (DHI, 2005). The HD module is based on the depth-averaged Saint-Venant equations that describe the evolution of the water level and two Cartesian velocity components, u and v, of which solutions are numerically obtained from a finite difference form of the equations (Warren and Bach, 1992; DHI, 2005). Although complex physical factors can affect flow dynamics in the real world and be implemented in MIKE 21, several assumptions were made in this study to simplify the HD model by considering dominantly impacting factors in this low-gradient treatment wetland setting. In this study, simplified forms of the fully dynamic equations were used based on the following assumptions:

- Bathymetry was fixed.
- Manning's roughness coefficient, which originally applied to steady uniform flow, was used as a lumped parameter of most hydraulic resistances generated in wetlands, including drag effect by vegetation stems, leaves and litter, as well as bottom surface roughness. In

this study, other approaches, such as Kadlec's equation (Kadlec and Knight, 1996; Kazezyilmaz-Alhan *et al.*, 2007) and depth-dependent Manning's equation (the coefficient as a function of water depth) (SFWMD, 2005), were not adapted because of the limitation of modelling platform.

- Coriolis effect, surface resistance by wind and shear stresses by turbulence are ignored.

Wind or wave action in shallow aquatic bodies sometimes plays a critical role in sediment dynamics (Chen, 1994; Langevin *et al.*, 2005); however, this effect can be minimized in densely vegetated constructed wetland systems like EAV treatment cells because emergent vegetation dampens wave energy and shelters the water surface from wind stress (Nepf, 1999; Braskerud, 2001). In addition, it was reported that SAV was effective in limiting wind-driven sediment and associated nutrient resuspension (Dennison *et al.*, 1993; Barko and James, 1997; Horppila and Nurminen, 2003). Hence, wind and wave action were not considered in this modelling study.

The surface flow regime in typical Florida wetlands is generally regarded as laminar to transient (Lee *et al.*, 2004) due to the low topographic slope, shallow water depth, dense herbaceous vegetation and subsequent slow flow velocity. Therefore, turbulence generated by flow velocity or vegetation is not considered a dominant process in the wetland systems (Harvey *et al.*, 2005; Leonard *et al.*, 2006) and included in modelling efforts (Lal, 1998; SFWMD, 2005). The impact of eddy viscosity on flow dynamics and mass transport was assumed to be negligible (set to zero).

The AD module is used to simulate transport of solutes. The AD equation was numerically solved using a third-order explicit finite difference scheme, QUICKEST (Ekebjaerg and Justesen, 1991). The dispersion coefficients in x and y directions are among the most important parameters in the AD module. To determine them, both directional dispersivities were estimated. In this case, the dispersion coefficients are changed continuously during the entire simulation period in accordance with the flow velocities calculated by the HD module at each simulation time step. The details of numerical algorithm and solution technique applied in the AD model are described in Ekebjaerg and Justesen (1991).

Data used in model

The hydrometeorological data of STA 5 northern flow way used in the HD model, including water level, flow, rainfall and evapotranspiration (ET), were collected by SFWMD and are available from the online environmental database, DBHYDRO (http://my.sfwmd.gov/dbhydropl sql/show_dbkey_info.main_menu). Daily rainfall data were collected onsite at G343B and daily hydrometeorological data measured from a nearby monitoring station in STA 1 W, located approximately 53 km to the northeast of study area, were used to estimate ET, based on a prediction equation suggested by Abtew (1996). The daily averaged water level and flow data were available for most hydraulic structures around the flow way, but not for all of the monitoring stations (G343A-D) located in the middle levee (only head- and tailwater levels of G343B and G343C were available). The flow data measured at the three input hydraulic structures (G342A, G342B and G349A) and two output hydraulic structures (G344A and G344B), plus rainfall/ET data were used as model input data, and the water level data measured at the most hydraulic structures were used for model calibration, validation and sensitivity analysis. Time series of rainfall, ET, and surface water inflow and outflow during the entire HD model simulation period (2·67 years) are presented in Figure 2.

Chloride data used in the AD model were also collected by SFWMD and downloaded from DBHYDRO. In this study, chloride was selected as a solute for a conservative transport simulation in that it was the most common non-reactive element of which concentration was reported biweekly at almost every water quality monitoring station. Time series chloride concentration data measured at three input points were used as a model input (Figure 3), and those measured at the middle levee (G343B and G343C) and output structures (G344A and G344B) were used for model calibration, validation and sensitivity analysis.

Water budget

The water budget of STA 5 northern flow way is comprised of the following components:

$$\Delta S = P - \mathrm{ET} + I_{\mathrm{SF}} - O_{\mathrm{SF}} - \mathrm{GW} + R \qquad (1)$$

where ΔS is storage change in wetland, P is rainfall, ET is evapotranspiration, I_{SF} is surface water inflow through culverts and pump station, O_{SF} is surface water outflow through culverts, GW is net groundwater seepage out and R is water budget error. Rainfall and ET values were multiplied by the model domain area (8 140 000 m^2) to obtain volume-based rainfall or ET for a certain period of time. No direct measurement of net groundwater seepage flow was made. Although Parrish and Huebner (2004) and Liyanage and Huebner (2005) used a linear equation with seepage coefficient to compute the groundwater seepage rate in STA 5, the single unknown component was determined as a residual of Equation (1) by setting the water budget error to zero in this study.

The water budget for study period is shown in Table II. Surface water inflow through G342A, G342B and G349A constitutes 93·2% of the total inflow. Rainfall is 6·8% of total inflow. Surface water outflow through G344A and G344B is 88·4% of total outflow. ET and seepage losses are estimated to be 7·4 and 4·2%, respectively. For details on estimation of water budget components through hydrometeorological monitoring at STA 5, refer to Liyanage and Huebner (2005).

Model configuration

Although the northern flow way of STA 5 was flooded in 1999, performance data for the first 3 years were not

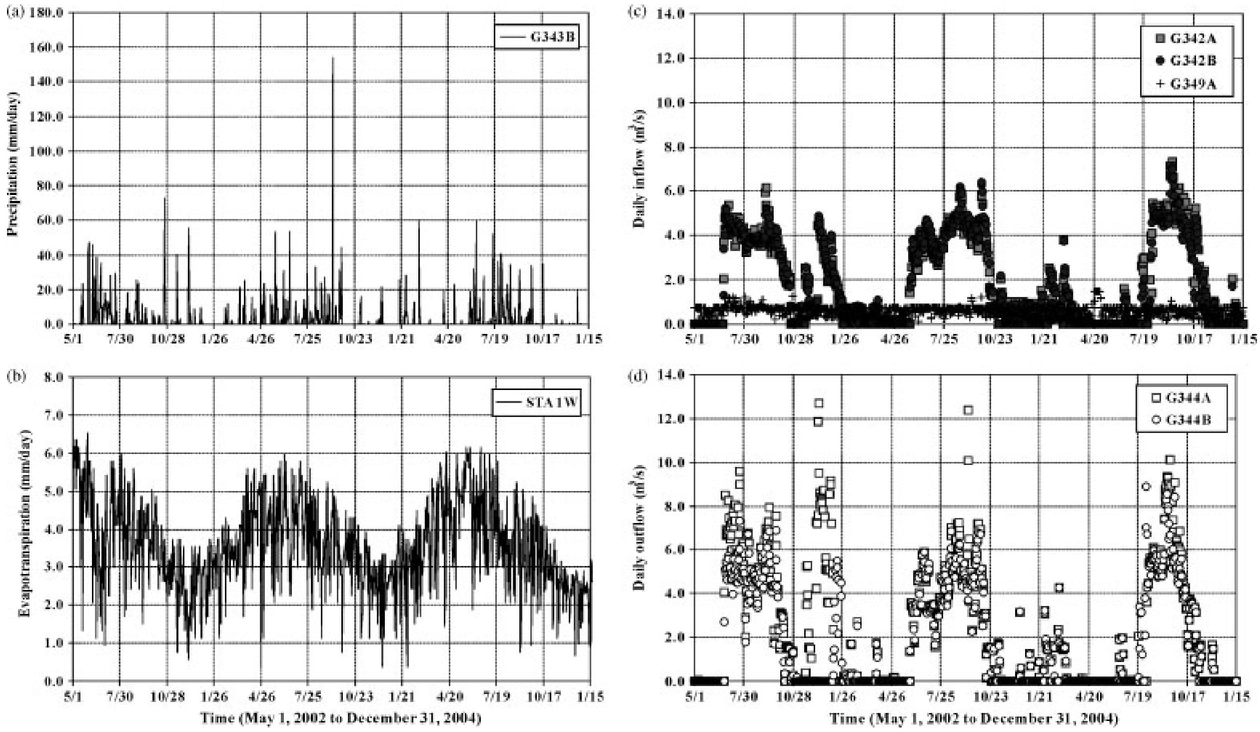

Figure 2. Time series (daily based) HD model input data. (a) Precipitation. (b) Evapotranspiration. (c) Surface inflows. (d) Surface outflows

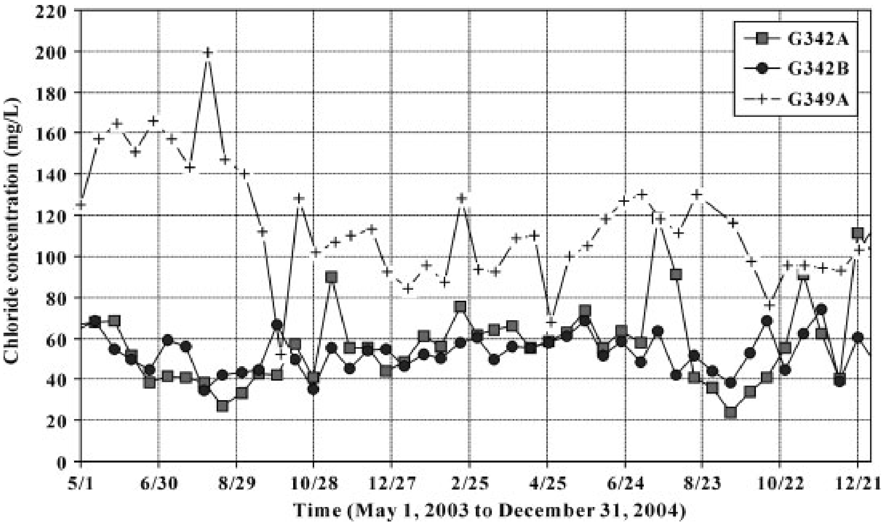

Figure 3. Time series AD model input data: Inlet chloride concentration profiles

Table II. Water budget for the HD simulation period

Dates	P	I_{SF}	$\sum$Inflow	ET	O_{SF}	GW	$\sum$Outflow	ΔS
May 2002 to April 2003	9·8	127·6	137·4	10·6	124·4	3·5	138·5	−1·1
May 2003 to April 2004	9·4	135·6	145·0	10·6	121·6	11·8	144·0	1·0
May 2004 to December 2004	6·8	92·8	99·6	7·1	89·4	3·6	100·2	−0·6
Total	26·0	356·0	382·0	28·3	335·4	18·9	382·7	−0·7
$\sum$Inflow or $\sum$Outflow (%)	(6·8)	(93·2)	—	(7·4)	(87·6)	(4·9)	—	—

P, precipitation; I_{SF}, surface water inflow; ET, evapotranspiration; O_{SF}, surface water outflow; GW, net groundwater seepage; ΔS, change in storage volume. Unit: 1 000 000 m^3.

analysed in this study because the interval was usually considered a period for start-up processes like vegetation colonization (Juston and DeBusk, 2006). The simulation period for HD model calibration is from 1 May 2002 to 30 April 2003 (1 year) and the simulation period for the model validation starts on 1 May 2003 and

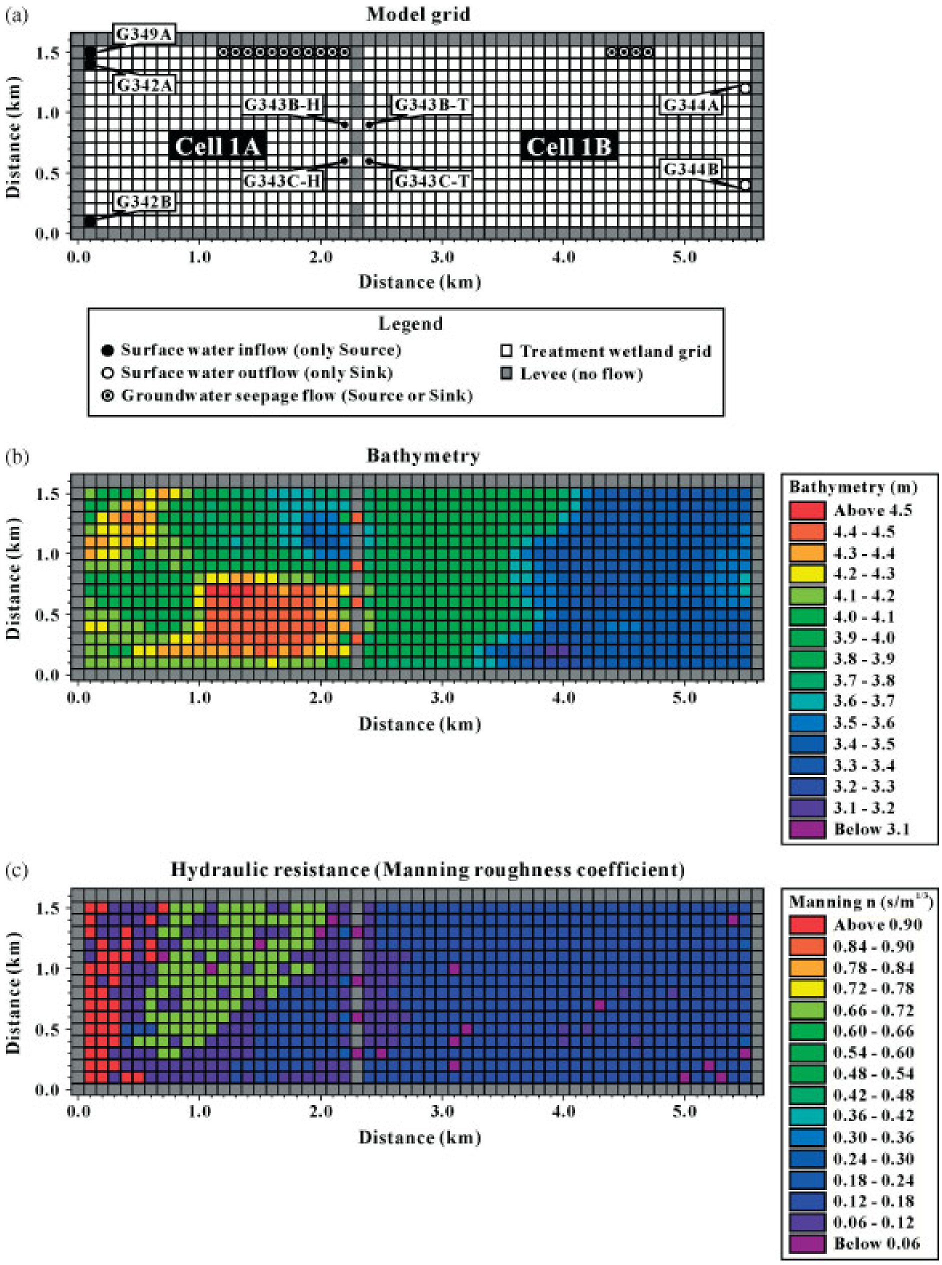

Figure 4. The model domain and spatially distributed model input data. (a) The model grid showing the location of surface water level monitoring stations and arrangement of grid cells for net seepage flow. (b) The raster-based bathymetry prediction map used in the model. (c) The hydraulic resistance (Manning's roughness coefficient) used in the model

ends on 31 December 2004 (1·67 years). Recent flow data after 1 January 2005 were not also considered for model simulation because the northern flow way was temporarily taken off-line from January 2005 to improve the mid levee hydraulic structures (Pietro *et al*., 2006). The simulation time step was 1 min.

For this study, the latest STA 5 topographic survey data (Wantman Group, Inc., 2005) was provided by the SFWMD; 216 georeferenced bathymetry measurement points (NGVD29) were interpolated using an inverse-distance weighting scheme to generate a continuous bathymetry prediction map for the study area. The average bathymetry elevation in Cell 1A (only effective treatment area) was 4·08 m and the average ground elevation in Cell 1B was 3·61 m. The bathymetry of the modelled area was formed on a 100 × 100 m grid (Figure 4a) and the raster-based bathymetry prediction map used in the model is illustrated in Figure 4b.

HD module setup. MIKE 21 requires specification of either the water surface elevation or the flux at all open boundary points. Unlike other aquatic bodies, surface inflows and outflows in most constructed wetlands are regulated by point source/sink-type hydraulic structures such as pump stations, weirs and culverts. Hence, the model boundary was closed to represent the berm around treatment wetland cells in this study (no surface flow at boundary), and the inflows and outflows were instead specified using the 'source and sink' option at each grid cell corresponding to the location of inflow and outflow hydraulic structures (Somes *et al.*, 1999; Min and Wise, 2009). Also, the source and sink option was used to represent net groundwater exchange, estimated as a residual term of water budget analysis.

Considering the location of the inflow hydraulic structures (G342A and G342B) and the seepage return pump (G349A), three point isolated source grid cells were assigned on the left side of the model domain to incorporate the rate, velocity and direction of inflow (Figure 4a). Note that a western area of the flow way surrounded by the distribution canal was excluded in the model domain because the topographically high area was not considered an effective treatment area. During the simulation period, daily averaged flow rates were divided by flow passing area of hydraulic structures to calculate daily average velocities. Likewise, two point isolated sink grid cells were assigned on the right side of model domain to incorporate the outflow (Figure 4a). Liyanage and Huebner (2005) reported that a net seepage loss was dominant in the entire flow way. The main seepage flow direction was out of the treatment cells towards the northern seepage canal and the discharge canal along the eastern boundary. Although there was no direct option for groundwater–surface water interaction in MIKE 21, 15 grid cells with low elevation (to avoid mass balance error due to dry out in high elevation areas) along the northern boundary of the flow way were assigned as point source/sinks to reflect net groundwater seepage flow in this modelling study (Figure 4a). Considering the expected higher head difference between the treatment cell and seepage canal in Cell 1A compared to Cell 1B, the greater number of grid cells was assigned to Cell 1A (11) than Cell 1B (4).

One of the main characteristics of the MIKE 21 flow model is that flooding and drying conditions of wetland can be represented with respect to the change of hydroperiod using a 'flood and dry' option. According to SFWMD (2005), detention depth is defined as a ponding depth at a grid cell below which no water transfer into the adjacent grid cell is allowed even if a hydraulic gradient exists. In the South Florida Water Management Model (SFWMM) model, around 0·03 m was suggested for the depth in various wetland types. Likewise, in the MIKE 21 HD module flooding and drying depths were assigned. Above the flooding depth, hydraulic roughness-controlled water flow was horizontally transferred along the hydraulic gradient; however, below the flooding depth, water did not move even if a hydraulic gradient existed. If water depth was less than the drying depth, the grid cell was considered to be a completely dried area. Flooding depth of 0·03 m and drying depth of 0·001 m, respectively, were selected in this study.

Water levels observed at nine measurement points within the northern flow way on the simulation starting date (1 May 2002) were linearly interpolated to set the initial condition for water level of the model domain. The differences in water levels within Cells 1A and 1B were about 0·08 and 0·04 m, respectively. About 0·3 m of abrupt water level decrease was observed between headwater and tailwater elevation of hydraulic structures located in the middle levee separating Cells 1A and 1B. Water levels of the Canal L-2 and discharge canal and the relationships to treatment cells were not modelled in this study. Time series monthly averaged groundwater seepage flows, estimated as a residual of the water budget, were divided by the number (15) of the grid cells assigned for the seepage flow and equally assigned to each grid cell. In other words, short-term (daily or weekly level) temporal and spatial variations of groundwater seepage flow within the model domain were not considered in this study. Rainfall and ET data were homogeneously assigned to every grid cell of the model domain.

Since hydraulic resistance, commonly represented as Manning's roughness coefficient, is closely related to vegetation type/density and water depth, it is spatio-temporally varied. Because of the model limitation, hydraulic resistance was assumed to be independent of any change in water depth in this study. That is, it was considered temporally constant. Hence, it was described only as a function of vegetation type (Langevin *et al.*, 2005). Based on a geographic information system (GIS) shapefile for vegetation distribution of the STA 5 northern flow way (Nick Miller, Inc., 2006), the vegetation of the study area was classified into five different categories. Table I shows the dominant vegetation species and coverage ratios. Although there are few good references on selection of the value for vegetation-covered areas in 2D HD models (Sutron Corp., 2005), literature-based Manning's coefficients were initially assigned to each reclassified class and finally determined by model calibration. Figure 4c illustrates the spatial distribution of Manning's coefficients used in the HD model; they are assigned at every grid cell of Cells 1A and 1B as a function of vegetation type.

AD module setup. AD simulation was performed for the period of 1 May 2003 to 31 December 2004 (1·67 years), which corresponded to the validation period of the HD model. This simulation period was selected considering the availability and seasonal fluctuation patterns of chloride data measured at all monitoring sites. Since the AD model was integrated with the HD model, it was first required to recalibrate the HD model to minimize the AD simulation error caused by the HD simulation error. For this, monthly averaged net groundwater seepage flows were slightly modified to generate the best HD model fit during the AD simulation period. The average HD model prediction error with adjusted seepage was approximately 0·11 m, and the water level simulation results of the recalibrated HD model are presented in Figure 5.

Chloride concentrations were monitored at seven hydraulic structures in STA 5 northern flow way (G342A, G342B, G349A, G343B, G343C, G344A and G344B). For specifying the initial chloride concentration of the study area, concentrations observed at the seven water quality measurement points on the simulation starting

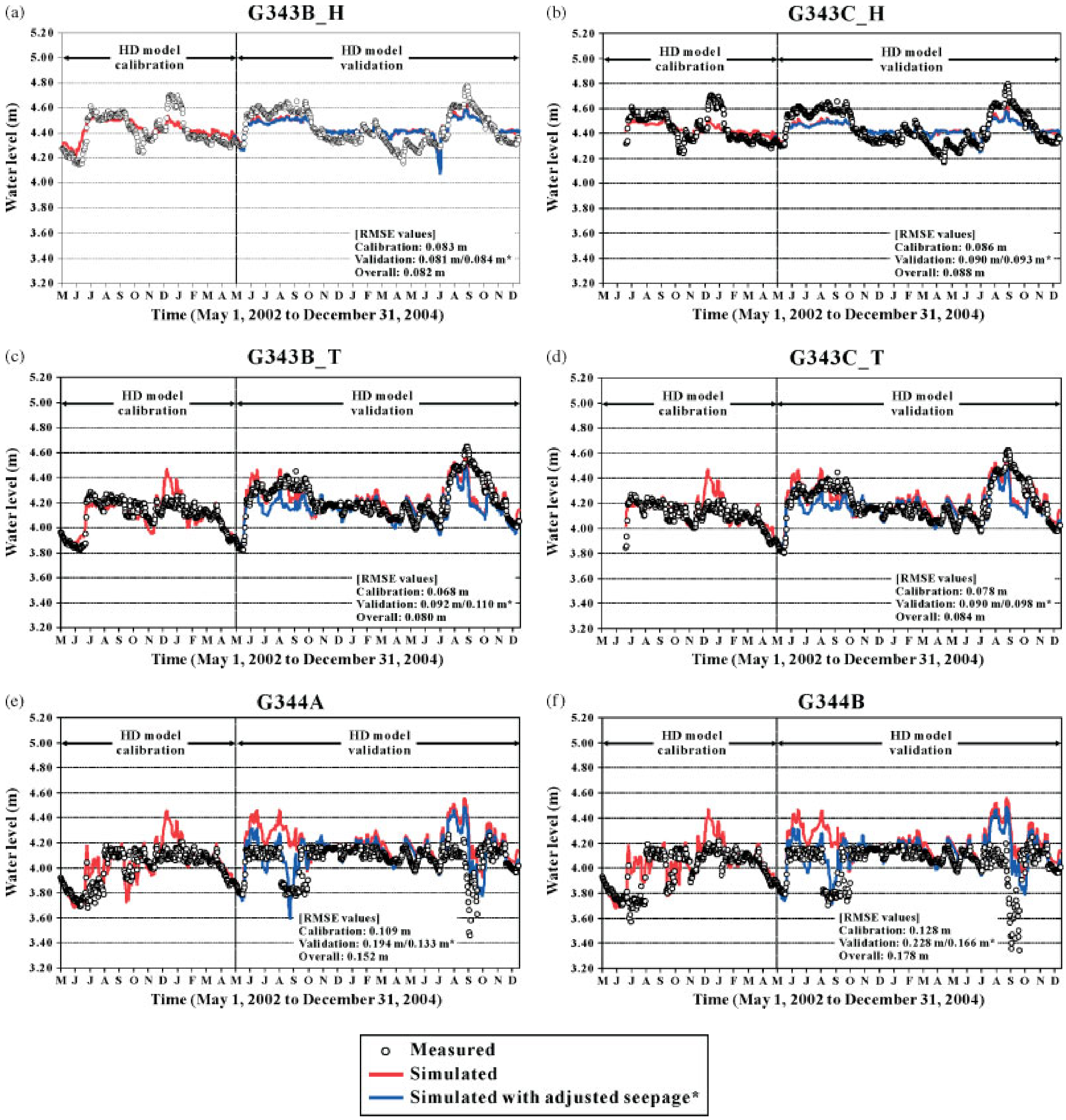

Figure 5. The HD model calibration and validation results on water level fluctuations at the six monitoring sites: (a) G343B_H, (b) G343C_H, (c) G343B_T, (d) G343C_T, (e) G344A and (f) G344B

date (1 May 2003) were linearly interpolated to generate the 2D continuous map. Time series profiles of inlet chloride concentration measured at G342A, G342B and G349A (Figure 3) were incorporated at each point source grid cell. In this model, to represent the atmospheric input of chloride by rainfall, a spatio-temporally constant chloride concentration of 1 mg/l (Hendry and Brezonik, 1980) was set as the rainfall concentration. Dispersion coefficients in x and y directions were determined as a time-varying parameter according to the change of flow velocity at each time step. In this case, dispersivities in x and y directions (α_x and α_y) should be specified. As the main flow direction is parallel to the x axis, the α_x and α_y are equal to the longitudinal (α_L) and transverse dispersivity (α_T) in this study. As an initial guess, dispersivities of 0·5 and 0·05 m were assigned in x and y directions ($\alpha_x : \alpha_y = 10:1$), respectively, and were finally determined by model calibration ($\alpha_x = 2$ m and $\alpha_y = 0{\cdot}1$ m; the ratio is about 20 : 1). The parameter estimation will be discussed later in this article.

Model calibration and validation

The HD model calibration was performed using six historic stages (G343B_H, G343B_T, G343C_H, G343C_T, G344A and G344B; Figure 4a) in the STA 5 northern flow way. For the AD model, it was performed with the time series profiles of chloride concentration observed at four observation points (G343B, G343C, G344A and G344B) in the study area. In this study, model calibration was accomplished by calculating the average value of root-mean-square errors (RMSEs) between measured and simulated data among the multiple observation sites. The calibration process objective was to minimize the average RMSE value:

$$\mathrm{RMSE} = \sqrt{\frac{\sum_{i=1}^{n}(S(t_i) - M(t_i))^2}{n}} \quad (2)$$

where $S(t_i)$ and $M(t_i)$ indicate simulated and measured data at a time step (t_i), respectively, and n is the number of total data during a simulation period. The calibrated HD and AD models were validated with each independent time series dataset, and the model prediction was evaluated with the same metric, RMSE.

Sensitivity analysis

After obtaining the best model fit between simulated and measured data by tuning model parameters, model sensitivity analysis on key model parameters was carried out. The sensitivities of simulated water levels (in the HD model) and chloride concentration profiles (in the AD model) at the monitoring points of study area to the key model parameter (hydraulic roughness coefficient (n) in the HD model and dispersivities (α_x and α_y) in the AD model) were examined. The parameter values estimated by the model calibration were used as baseline values. In each sensitivity run, only a single model parameter was changed within a certain range. In this study, the sensitivities of average water levels to the overall $\pm30\%$ changes of estimated n values were evaluated using the sensitivity coefficient defined as $S_{h,n} = \frac{\Delta h/h}{\Delta n/n}$ and the sensitivities of chloride concentration profiles to the changes of estimated α_x and α_y values were deduced during model calibration.

RESULTS AND DISCUSSION

Spatio-temporal variation in water level

Understanding spatio-temporal variation in water level in a constructed wetland system plays a key role in optimizing management and maximizing treatment efficiency. In this study, time series simulated water level profiles, extracted from two grid cells corresponding to the headwater measurement points (G343B_H and G343C_H) of two hydraulic structures located at the middle levee, were compared to the measured data to verify simulation results of the HD model in Cell 1A. Likewise, simulation results in Cell 1B were verified by comparing measured data with simulated water level profiles extracted from four grid cells corresponding to the tailwater measurement points (G343B_T and G343C_T) of two hydraulic structures at the middle levee and headwater measurement points (G344A_H and G344B_H) of two outlet hydraulic structures at the downstream levee.

Figure 5 illustrates the simulation results of the HD model on water level fluctuation at the six water level measurement points during the model calibration and validation period. Spatio-temporal variation in water level in the flow way was simulated well; the average annual model calibration error on six measured water level profiles was approximately 0·09 m. Average simulation RMSE of the HD model in Cell 1A (0·085 m) was less than that in Cell 1B (0·096 m). Although few deviations were observed in any short period (e.g. December 2002), simulation results on the general water level showed a decreasing pattern from upstream to downstream, and timing and intensity of water level peaks at each monitoring point agreed very well with those of observed data.

The spatio-temporal variation of water level was also predicted using an independent dataset of 1·67 years. As illustrated in Figure5, simulated water level profiles in Cell 1B, particularly at G344A and G344B, are slightly overestimated through the entire simulation period. This indicates that the real groundwater seepage loss in Cell 1B may be slightly higher than the amount estimated as the monthly averaged water budget residual. In reality, this overestimated pattern was not observed when the groundwater seepage loss was adjusted (mostly increased) to obtain the best HD model fit during the validation period (Figure 5).

As discussed by Min and Wise (2009), topographical heterogeneity in bathymetry is one of the primary factors causing uneven flow pathways in a wetland system. A topographically high elevation area located ahead of G343C was dry or very shallow even in storm season (Figure 4b). Although no obvious major short-circuiting flow pathways were observed, it was obvious that some locally high surface elevation areas, which experience frequent dry-outs, contribute to generate the spatial differences of time series data profiles (water quality as well as water level) among the monitoring points. In this study, small variations of model prediction errors among the six water level observation points indicated that this 2D HD model was spatially well balanced enough to catch differences of 2D data formed by the spatial heterogeneity of physical settings like bathymetry and vegetation distribution. All results also reveal that the water level of constructed wetlands can be successfully simulated through the simple applications of a source/sink option in the MIKE 21 HD model rather than by complex boundary specification processes.

Hydraulic resistance

Theoretical approaches to the flow dynamics in free surface natural or constructed wetlands do not have a long history compared to other surface water flow systems. Most theories originated from open channel hydraulics. However, there are still many controversial issues unresolved in describing the flow dynamics by applying

Table III. Manning's roughness coefficients used in the HD model

Type of vegetation habitat	Dominant coverage (%)	Manning's n (s/m$^{1/3}$)
Emergent	0·5–6·6	0·67
Floating	0·02–0·031	0·12
Shrub	1·75–2·6	1·00
Open water with or without vegetation	0·21–0·34	0·12
Open water with *Hydrilla*	4·0–26·5	0·15
Hydraulic structure (culvert)	—	0·024

Table IV. Sensitivity of water level to the change (±30%) in hydraulic resistance (Manning's roughness coefficient)

Water level monitoring stations	Baseline annual average water level (m)	Sensitivity coefficient, $S_{h,n}$	
		+30% of Manning's n	−30% of Manning's n
G343B_H	4·43	0·008	0·005
G343B_T	4·10	0·021	−0·014
G343C_H	4·42	0·006	0·003
G343C_T	4·11	0·018	−0·013
G344A	4·03	0·002	−0·041
G344B	4·04	0·008	−0·038

existing theories to free surface wetland systems. One of these is how to estimate the hydraulic resistances of vegetation-covered areas. Free surface water movement in natural or constructed wetlands, sometimes called sheetflow or overland flow, is usually governed by the hydraulic resistance of the vegetation. Manning's roughness coefficient is commonly used to quantify a lumped hydraulic resistance caused by bottom sediment and vegetation stem/litter friction. Over the model domain, 2D map-typed values were assigned as a function of vegetation type.

Coefficient values were initially selected considering the range of Manning's roughness coefficient values suggested in previous literature data (Kadlec and Knight, 1996; SFWMD, 2005; Sutron Corp., 2005; Min and Wise, 2009) and finally determined through the HD model calibration to the historic stage data observed in the study area, as shown in Figure 5. Manning's roughness coefficients determined in this flow way are summarized in Table III. For dense EAV and SAV areas, 0·67–1·0 and 0·12–0·15 s/m$^{1/3}$, respectively, of the roughness coefficient ranges were estimated in this study.

Effective roughness value (N) defined in the SFWMD (2005), which is similar to Manning's coefficient, was compared with the estimated ones. The N values are calculated as a function of land use (wetland) type and water depth. In the case of a cattail-dominant wetland, 0·70 s/m$^{1/3}$ is suggested when a ponding depth of a grid cell is 0·61 m (nominally 2 ft). In the 2D hydraulic modelling study of STA 5 executed by Sutron Corp. (2005), 0·5–1·3 and 0·3–0·8 s/m$^{1/3}$ of the roughness coefficient values were assigned with the change of water depth from 0·15 to 0·91 m (nominally 0·5–3·0 ft) on cattail and SAV-dominant treatment cells, respectively. Although it is not easy to compare Manning's roughness coefficient values estimated in this study directly with the historically reported roughness data, parameter values estimated by model calibration were not significantly different from the ranges suggested by SFWMD (2005) and Sutron Corp. (2005).

HD model sensitivity analysis

A sensitivity analysis was completed to investigate the range of water level sensitivity due to ±30% variation in Manning's roughness coefficient (Table IV). A 30% increase of Manning's roughness coefficients caused an average difference of 0·01 m in water level at the six measurement points (0–0·03 m); conversely, a 30% decrease of the coefficients brought about an average difference of 0·02 m in water level (0–0·05 m). When Manning's roughness coefficient values varied by ±30%, water level variations in Cell 1B (G343B_T, G343C_T, G344A, and G344B) were higher than in Cell 1A (G343B_H and G343C_H). Although we can say that the water level in the SAV system is more sensitive to changing hydraulic resistance than that in the EAV dominant system, the absolute significance was not critical because all these differences were much smaller than the average simulation error (about 0·1 m).

Chloride transport

Figure 6 shows the simulation results of the AD model on chloride concentration profiles at the four water quality measurement points in the flow way during the model calibration (1 May 2003 to 30 April 2004) and validation period (1 May 2004 to 31 December 2004). In this study, time series simulated chloride concentration profiles extracted from the grid cells corresponding to G343B and G343C were compared to measured data to verify simulation results of the AD model in Cell 1A. Likewise, simulation results in Cell 1B were verified by comparing measured data with simulated chloride concentration profiles extracted from the grid cells corresponding to G344A and G344B. Simulated results of chloride concentration profiles agreed well with measured data during the entire simulation period. The average values of model calibration and validation errors at the four measurement points were 13·48 and 13·66 mg/l, which corresponded to about 14·6 and 15·3%, respectively, as a percent model error, defined as RMSE divided by the range of the measured data. The simulation errors in Cell 1A (average 9·62 mg/l) were less than those in Cell 1B (average 17·33 mg/l), which may be partially due to the greater HD simulation errors in Cell 1B (Figure 5). These remarkable calibration and validation results of the AD model ensure the robustness of the HD model as well as the AD model.

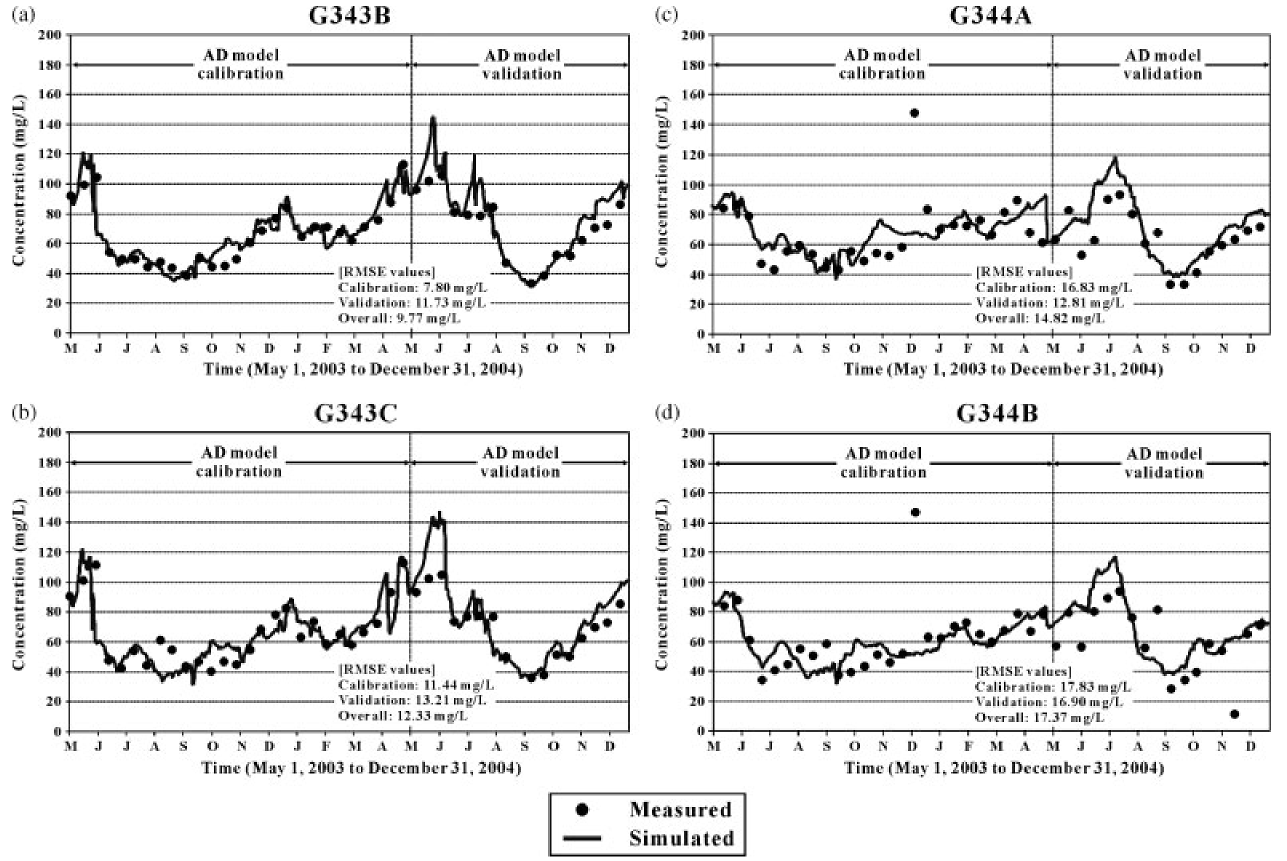

Figure 6. The AD model calibration and validation results on chloride concentration profiles at the four monitoring sites: (a) G343B, (b) G343C, (c) G344A and (d) G344B

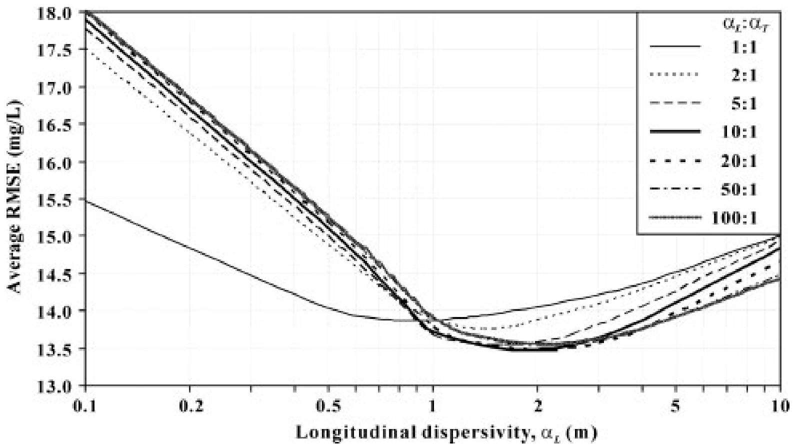

Figure 7. Chloride transport model calibration curves of longitudinal and transverse dispersivity

Longitudinal and transverse dispersivity

Calibration results of the chloride transport AD model with respect to the ratio of longitudinal (x direction; α_L) versus transverse dispersivity (y direction; α_T) in STA 5 northern flow way are shown in Figure 7. The curves in the figure were delineated on the basis of the results during the model calibration effort at the four chloride monitoring stations. In the case of the curve with the ratio of 1 : 1 between α_L and α_T, it had the lowest average RMSE value, 13·87 mg/l, when α_L was around 0·9. As the ratio of α_L and α_T gradually increased to 20 : 1, the lowest average RMSE value of each calibration curve decreased to 13·48 mg/l. However, once the ratio was greater than 20 : 1, the lowest RMSE value starts to increase again. As shown in Figure 7, the curves have the minimum average RMSE value when α_L is around 2 m, although there are very slight differences among the curves. This suggests that the average RMSE of chloride transport simulation has the lowest value (13·48 mg/l) when α_L is 2 m and the ratios of α_L and α_T are 10 : 1 or 20 : 1. Hence, model-based longitudinal and transverse dispersivities of 2 and 0·1 m, respectively, on the whole flow way were determined through the model calibration.

Using the estimated dispersivities in x (2 m) and y directions (0·1 m), ranges of model-based dispersion coefficients (D_x and D_y) in the STA 5 northern flow way were estimated on the basis of ranges of x and y directional flow velocities (u and v). According to HD simulation results on the study area, x and y directional flow velocities had the minimal value, zero, when water was stagnant and had a maximum value of 0·14 m/s in the hydraulic structure. Rather than using these extreme flow velocity conditions, it seemed reasonable to use a range to represent the change of flow velocity within the treatment cells (0·001–0·05 m/s). Considering the practical range of flow velocity, the ranges of 2D, spatially distributed model-based D_x and D_y were estimated from 0·002 to 0·1 and 0·0001 to 0·005 m^2/s, respectively. Compared to previous results ranging from a small-scale flume experiment to larger scale pilot tests or 1D transport models, we conclude that the estimates in this study were determined reasonably. With a 1D solute transport model with transient storage, Martinez and Wise (2003) and Keefe *et al.* (2004) reported a similar range of longitudinal dispersion coefficient values in constructed wetlands (0·010–0·512 and 0·0025–0·0213 m^2/s, respectively). In addition, Ho *et al.* (2009) reported a range of longitudinal dispersion coefficients (0·037–0·26 m^2/s) through pilot experiments (<1 km) in the Florida Everglades. Conversely, the model-derived values were generally higher than the ranges from smaller scaled, flume-based tracer experiments in the South Florida wetland (0·00002–0·00484 m^2/s) (Saiers *et al.*, 2003; Huang *et al.*, 2008), which can be explained by the scale dependency (Ho *et al.*, 2009). In this study, the systematic impacts of changes in cell size on the estimated dispersion coefficients were not tested. Hence, further modelling studies are required to evaluate how the parameter estimation process is affected by the changes in model grid size.

These results show that the assumption of a homogeneous and isotropic dispersion coefficient, which is commonly assumed in 2D surface water solute transport models, may cause a significant error in representing the dispersive characteristics in constructed wetlands, in particular, at treatment wetland systems the coordinate of which is parallel to the main flow direction. Also, the quantitative difference of dispersivity between the EAV and SAV systems was not evaluated independently by model calibration in this study because the AD model enforced only single x- and y-directional dispersivity value through the entire model domain. Therefore, the estimates represent the overall effect of an EAV–SAV integrated flow way, so direct application of these values to other constructed wetland settings should be made with caution. Future sampling and modelling efforts are needed to systematically examine the difference in model-based dispersivities (dispersion coefficients) between two dominant types of treatment wetland.

AD model sensitivity analysis

Sensitivities of the chloride concentration profiles to the changes of longitudinal and transverse dispersivity were examined. The AD model sensitivities on the change of α_L (0·1–10 m) and α_T (0·02–2 m) when α_T is fixed at 0·1 m and α_L is fixed at 2 m, respectively, were deduced during the model calibration (Figure 7). Compared to the baseline value of 13·48 mg/l as the average RMSE value, the differences from the baseline value in the average RMSE values were generally higher in sensitivity tests on α_L (up to 2 mg/l) than α_T (up to 0·5 mg/l). This reveals that longitudinal dispersivity is a more sensitive parameter than the transverse one in the AD model, a not surprising result.

Since the main flow direction was almost parallel to the x axis of model domain in this study, α_x and α_y were identical to longitudinal and transverse dispersivity. However, modellers should be careful in directly applying values or ranges suggested in this study to other constructed wetland systems because the axis of model domain is not always parallel to the main flow direction. If parallel, it could save time and effort for model calibration to consider the effect of transverse dispersivity after calibrating a model first with respect to the longitudinal dispersivity. Also, the relatively small variations of dispersivities in sensitivity tests imply that advective transport is dominant in this treatment flow way rather than dispersive transport, which may be a reason for the poor phosphorus removal efficiency (mass removal rate of 46%), as reported by Juston and DeBusk (2006), compared to the other treatment flow ways, because it can cause relatively low effective treatment area (high dead zone) and short hydraulic residence time.

SUMMARY

A 2D, spatially distributed flow dynamic and solute transport model was developed using MIKE 21 HD and AD modules as the basic framework and tested against field data monitored at the northern flow of STA 5. In this study, the spatio-temporal variations of water level fluctuations and chloride concentration profiles were reasonably simulated through a linkage between the HD and AD modules, and key model parameters were estimated.

The model incorporated time-varying, daily based measurements of such water budget components as stage, flow, rainfall and ET, and monthly averaged net groundwater seepage was determined through an effort to minimize the monthly water budget error. GIS-based analyses were carried out to estimate and map bathymetry and hydraulic resistance. In this model, groundwater flows as well as surface flows through hydraulic structures were described simply by using a point source/sink option.

The results of HD model calibration (1 year) and validation (1·67 years) on the water level profiles observed in the field demonstrate that the spatio-temporal changes of water level in the study area were reasonably simulated. The average annual model prediction error on six measured water level profiles was less than 0·10 m. Through the model calibration process, ranges of Manning's roughness coefficient for each vegetation habitat were also estimated as a function of vegetation type. For dense EAV and SAV areas, 0·67–1·0 and 0·12–0·15 s/m$^{1/3}$, respectively, of the roughness coefficient ranges are suggested in this study.

Integrated with the HD model, the AD model successfully simulates the spatio-temporal changes of chloride concentration profiles observed in the field with an average model error of about 15%. Through the AD model calibration, longitudinal dispersivity, estimated to be 2 m, was over an order of magnitude higher than the transverse one for the entire flow way. Based on parameter estimation, ranges of dispersion coefficients in longitudinal and transverse directions in the chained treatment cells are suggested ($D_L = 0{\cdot}002–0{\cdot}1$ m^2/s and $D_T = 0{\cdot}0001–0{\cdot}005$ m^2/s) and compared to literature values. Sensitivity test results show that the longitudinal dispersivity is a more sensitive parameter than the transverse one.

Based on the HD and AD modelling framework described in this article, various levels of phosphorus dynamic models will be linked and tested to develop a predictive tool for optimized management of constructed wetlands.

ACKNOWLEDGEMENTS

The authors thank the DHI Corporation for providing access to and support for the software mentioned herein. J.-H. M thanks the University of Florida for providing financial support through an Alumni Fellowship. They are also indebted to two anonymous reviewers for insightful comments that improved an early version of the manuscript.

REFERENCES

Abtew W. 1996. Evapotranspiration measurements and modeling for three wetland systems in south Florida. *Water Resources Bulletin* **32**: 465–473.

Arnold JG, Allen PM, Morgan DS. 2001. Hydrologic model for design and constructed wetlands. *Wetlands* **21**: 167–178.

Barko JW, James WF. 1997. Effects of submerged aquatic macrophytes on nutrient dynamics, sedimentation, and resuspension. In *The Structuring Role of Submerged Macrophytes in Lakes—Ecological Studies*, vol. 131, Jeppesen E, Søndergaard MA, Søndergaard MO, Christoffersen K (eds). Springer: New York; 197–214.

Braskerud BC. 2001. The influence of vegetation on sedimentation and resuspension of soil particles in small constructed wetlands. *Journal of Environmental Quality* **30**: 1447–1457.

Chen XJ. 1994. *Effects of Hydrodynamics and Sediment Transport Processes on Nutrient Dynamics in Shallow Lakes and Estuaries*. PhD dissertation, University of Florida, Gainesville.

Chen XJ, Sheng YP. 2005. Three-dimensional modeling of sediment and phosphorus dynamics in Lake Okeechobee, Florida: Spring 1989 simulation. *Journal of Environmental Engineering: ASCE* **131**: 359–374.

Chimney MJ, Goforth G. 2001. Environmental impacts to the Everglades ecosystem: a historical perspective and restoration strategies. *Water Science and Technology* **44**(11–12): 93–100.

Conaway JS, Moran EH. 2004. *Development and calibration of a two-dimensional hydrodynamic model of the Tanana River near Tok, Alaska*. US Geological Survey Open-File Report 2004-1225, US Geological Survey: Reston; 21.

Cook CB, Richmond MC, Coleman A, Rakowski CL, Titzler PS, Bliech MD. 2003. *Numerically Simulating the Hydrodynamic and Water Quality Environment for Migrating Salmon in the Lower Snake River*. US DOE report PNNL-14297: Richland.

Cui J, Li C, Sun G, Trettin C. 2005. Linkage of MIKE SHE to Wetland-DNDC for carbon budgeting and anaerobic biogeochemistry simulation. *Biogeochemistry* **72**: 147–167.

Dennison WC, Orth RJ, Moore KA, Stevenson JC, Carter V, Kollar S, Bergstrom PW, Batiuk RA. 1993. Assessing water quality with submersed aquatic vegetation. *Bioscience* **43**: 86–94.

DHI. 2005. *MIKE 21 Flow Model Hydrodynamics Module—Scientific Documentation*, Danish Hydraulic Institute: Hørsholm, Denmark.

Ekebjaerg L, Justesen P. 1991. An explicit scheme for advection diffusion modeling in two dimensions. *Computer Methods in Applied Mechanics and Engineering* **88**: 287–297.

Feng K, Molz FJ. 1997. A 2-D, diffusion-based, wetland flow model. *Journal of Hydrology* **196**: 230–250.

Fernandez GP, Chescheir GM, Skaggs RW, Amatya DM. 2006. DRAINMOD-GIS: a lumped parameter watershed scale drainage and water quality model. *Agricultural Water Management* **81**: 77–97.

Ferrarin C, Umgiesser G. 2005. Hydrodynamic modeling of a coastal lagoon: the Cabras lagoon in Sardinia, Italy. *Ecological Modelling* **188**: 340–357.

Gearheart RA. 1999. The use of free surface constructed wetland as an alternative process treatment train to meet unrestricted water reclamation standards. *Water Science and Technology* **40**(4): 375–382.

Goforth GF. 2001. Surmounting the engineering challenges of Everglades restoration. *Water Science and Technology* **44**(11–12): 295–302.

Goforth GF. 2005. *Summary of STA Vegetation Management Practices*. South Florida Water Management District: West Palm Beach.

Guardo M, Fink L, Fontaine TD, Newman S, Chimney M, Bearzotti R, Goforth G. 1995. Large-scale constructed wetlands for nutrient removal from stormwater runoff: an everglades restoration project. *Environmental Management* **19**: 879–889.

Guardo M, Tomasello RS. 1995. Hydrodynamic simulations of a constructed wetland in South Florida. *Water Resources Bulletin* **31**: 687–701.

Hammer DA. 1989. *Constructed Wetlands for Wastewater Treatment: Municipal, Industrial, and Agricultural*. Lewis Publishers: Chelsea; 831.

Harvey JW, Saiers JE, Newlin JT. 2005. Solute transport and storage mechanisms in wetlands of the Everglades, south Florida. *Water Resources Research* **41**: W05009. DOI: 10.1029/2004WR003507.

Hendry CD, Brezonik PL. 1980. Chemistry of precipitation at Gainesville, Florida. *Environmental Science and Technology* **14**: 843–849.

Ho DT, Engel VC, Variano EA, Schmieder PJ, Condon ME. 2009. Tracer studies of sheet flow in the Florida Everglades. *Geophysical Research Letters* **36**: L09401. DOI: 10.1029/2009GL037355.

Horppila J, Nurminen L. 2003. Effects of submerged macrophytes on sediment resuspension and internal phosphorus loading in Lake Hiidenvesi (southern Finland). *Water Research* **37**: 4468–4474.

Huang YH, Saiers JE, Harvey JW, Noe GB, Mylon S. 2008. Advection, dispersion, and filtration of fine particles within emergent vegetation of the Florida Everglades. *Water Resources Research* **44**: W04408. DOI: 10.1029/2007WR006290.

Jawitz JW, Muñoz-Carpena R, Muller S, Grace KA, James AI. 2008. *Development, Testing, and Sensitivity and Uncertainty Analyses of a Transport and Reaction Simulation Engine (TaRSE) for Spatially Distributed Modeling of Phosphorus in South Florida Peat Marsh Wetlands*. USGS Scientific Investigations Report 2008–5029, USGS: Reston; 109.

Ji Z. 2008. *Hydrodynamics and Water Quality: Modeling Rivers, Lakes, and Estuaries*. John Wiley & Sons: Hoboken, New Jersey; 676.

Jin KR, Hamrick JH, Tisdale T. 2001. Application of three-dimensional hydrodynamic model for Lake Okeechobee. *Journal of Hydraulic Engineering: ASCE* **126**: 758–771.

Johnson BH, Kim KW, Heath RE, Hsieh BB, Butler L. 1993. Validation of a three-dimensional hydrodynamic model of Chesapeake Bay. *Journal of Hydraulic Engineering: ASCE* **119**: 2–20.

Juston J, DeBusk TA. 2006. Phosphorus mass load and outflow concentration relationships in stormwater treatment areas for Everglades restoration. *Ecological Engineering* **26**: 206–223.

Kadlec RH. 2000. The inadequacy of first-order treatment wetland models. *Ecological Engineering* **15**: 105–119.

Kadlec RH, Hammer DE. 1988. Modeling nutrient behavior in wetlands. *Ecological Modelling* **40**: 37–66.
Kadlec RH, Knight RL. 1996. *Treatment Wetlands*. Lewis Publishers: Boca Raton; 893.
Kazezyilmaz-Alhan CM, Medina MA Jr, Richardson CJ. 2007. A wetland hydrology and water quality model incorporating surface water/groundwater interactions. *Water Resources Research* **43**: W04434. DOI: 10.1029/2006WR005003.
Keefe SH, Barber LB, Runkel RL, Ryan JN, McKnight DM, Wass RD. 2004. Conservative and reactive solute transport in constructed wetlands. *Water Resources Research* **40**: W01201. DOI: 10.1029/2003WR-002130.
Kivaisi AK. 2001. The potential for constructed wetlands for wastewater treatment and reuse in developing countries: a review. *Ecological Engineering* **16**: 545–560.
Kronvang B, Hoffmann CC, Svendsen LM, Windolf J, Jensen JP, Dørge J. 1999. Retention of nutrients in river basins. *Aquatic Ecology* **33**: 29–40.
Lal AMW. 1998. Weighted implicit finite-volume model for overland flow. *Journal of Hydraulic Engineering: ASCE* **124**: 941–950.
Langevin C, Swain E, Wolfert M. 2005. Simulation of integrated surface-water/ground-water flow and salinity for a coastal wetland and adjacent estuary. *Journal of Hydrology* **314**: 212–234.
Lee JK, Roig LC, Jenter HL, Visser HM. 2004. Drag coefficients for modeling flow through emergent vegetation in the Florida Everglades. *Ecological Engineering* **22**: 237–248.
Leonard L, Croft A, Childers D, Mitchell-Bruker S, Solo-Gabriele H, Ross M. 2006. Characteristics of surface-water flows in the ridge and slough landscape of Everglades National Park: implications for particulate transport. *Hydrobiologia* **569**: 5–22.
Liyanage TR, Huebner RS. 2005. *Water budget analysis for Stormwater Treatment Area 5 (Water Year 2003–2004)*, Technical Publication ERA 427. South Florida Water Management District, South Florida Water Management: West Palm Beach.
Martinez CJ, Wise WR. 2003. Analysis of constructed treatment wetland hydraulics with the transient storage model OTIS. *Ecological Engineering* **20**: 211–222.
McMichael CE, Hope AS, Loaiciga HA. 2006. Distributed hydrological modelling in California semi-arid shrublands: MIKE SHE model calibration and uncertainty estimation. *Journal of Hydrology* **317**: 307–324.
Min JH, Wise WR. 2009. Simulating short-circuiting flow in a constructed wetland: the implications of bathymetry and vegetation effects. *Hydrological Processes* **23**: 830–841.
Mitsch WJ. 1994. *Global Wetlands: Old World and New*. Elsevier Science: Amsterdam, The Netherlands; 967.
Moustafa MZ, Hamrick JM. 2000. Calibration of the wetland hydrodynamic model to the Everglades Nutrient Removal Project. *Water Quality and Ecosystem Modeling* **1**: 141–167.
Nepf HM. 1999. Drag, turbulence, and diffusion in flow through emergent vegetation. *Water Resources Research* **35**: 479–489.
Newman JM, Lynch T. 2001. The Everglades Nutrient Removal Project test cells: STA optimization status of the research at the north site. *Water Science and Technology* **44**(11–12): 117–122.
Nick Miller, Inc. 2006. *STA 5 vegetation Map*. http://my.sfwmd.gov/gisapps/sfwmdxwebdc/dataview.asp?query=unq_id=1660 (Accessed on August 24, 2009).
Park K, Jung HS, Kim HS, Ahn SM. 2005. Three-dimensional hydrodynamic-eutrophication model (HEM-3D): application to Kwang-Yang Bay, Korea. *Marine Environmental Research* **60**: 171–193.
Parrish DM, Huebner RS. 2004. *Water budget analysis for Stormwater Treatment Area 5 (May 1, 2000 to April 30, 2003)*, Technical Publications EMA 418. South Florida Water Management District, South Florida Water Management: West Palm Beach.
Persson J. 2005. The use of design elements in wetlands. *Nordic Hydrology* **36**: 113–120.
Persson J, Somes NLG, Wong THF. 1999. Hydraulics efficiency of constructed wetlands and ponds. *Water Science and Technology* **40**(3): 291–300.
Pietro K, Bearzotti R, Germain G, Iricanin N. 2009. *STA Performance, Compliance, and Optimization*, Chapter 5. 2009 South Florida Environmental Report. South Florida Water Management District, South Florida Water Management: West Palm Beach.
Pietro KC, Chimney MJ, Steinman AD. 2006. Phosphorus removal by the Ceratophyllum/periphyton complex in a south Florida (USA) freshwater marsh. *Ecological Engineering* **27**: 290–300.
Saiers JE, Harvey JW, Mylon SE. 2003. Surface-water transport of suspended matter through wetland vegetation of the Florida everglades. *Geophysical Research Letters* **30**: 1987. DOI: 10.1029/2003GL018132.
SFWMD. 2000. *Operation Plan: Stormwater Treatment Area 5 (Revised)*. South Florida Water Management District: West Palm Beach.
SFWMD. 2005. *Final Documentation for the South Florida Water Management Model (SFWMM) v5.5*. South Florida Water Management District: West Palm Beach.
Somes NLG, Bishop WA, Wong THF. 1999. Numerical simulation of wetland hydrodynamics. *Environmental International* **25**: 773–779.
Sutron Corp. 2005. *STA 5 2-D Hydraulic Modeling (linked cells model)*, Task 4·3 Final report. South Florida Water Management District: West Palm Beach.
Swain ED, Wolfert MA, Bales JD, Goodwin CR. 2004. *Two-dimensional Hydrodynamic Simulation of Surface Water Flow and Transport to Florida Bay through the Southern Inland and Coastal Systems (SICS)*, U.S. Geological Survey Water Resources Investigations Report 03–4287, USGS: Tallahassee; 56.
Thompson JR, Sorenson HR, Gavin H, Refsgaard A. 2004. Application of the coupled MIKE SHE/MIKE 11 modelling system to a lowland wet grassland in southeast England. *Journal of Hydrology* **293**: 151–179.
Tsanis IK, Prescott KL, Shen H. 1998. Modelling of phosphorus and suspended solids in Cootes Paradise marsh. *Ecological Modelling* **114**: 1–17.
Van Nes EH, Scheffer M. 2005. A strategy to improve the contribution of complex simulation models to ecological theory. *Ecological Modelling* **185**: 153–164.
Wantman Group Inc. 2005. *Stormwater Treatment Area 5 Topographic Survey*. West Palm Beach.
Warren IR, Bach HK. 1992. MIKE 21: a modeling system for estuaries, coastal waters and seas. *Environmental Software* **7**: 229–240.
Zacharias I, Gianni A. 2008. Hydrodynamic and dispersion modeling as a tool for restoration of coastal ecosystems. Application to a re-flooded lagoon. *Environmental Modelling and Software* **23**: 751–767.

